# Assessing glacier melt contribution to river runoff at Universidad glacier, central Andes of Chile

Claudio Bravo[1], Thomas Loriaux[1,2], Andrés Rivera[1,3] , Ben W. Brock[4]

[1] Centro de Estudios Científicos, Valdivia, Chile.
[2] School of Earth Sciences, University of Bristol, Bristol, UK.
[3] Departamento de Geografía Universidad de Chile, Santiago, Chile.
[4] Department of Geography, Northumbria University, Newcastle, UK.

*Correspondence to:* Claudio Bravo (claudiobravo.lechuga@gmail.com)

**Abstract**. Glacier melt is an important source of water for high Andean rivers in central Chile, especially in dry years when it can be an important contributor to flows during late summer and autumn. However, few studies have quantified glacier melt contribution to river runoff. To address this shortcoming, we present an analysis of meteorological conditions and melt for Universidad glacier, a large valley glacier in the central Andes of Chile at the head of the Tinguiririca river, for the 2009-2010 ablation season. We used meteorological measurements from two automatic weather stations installed on the glacier to drive a distributed temperature-index melt and runoff routing model, and to compare total modelled glacier melt to river flow measurements at three sites located between 0.5 and 50 km downstream. The temperature-index model was calibrated at the lower weather station site and showed good agreement with melt estimates from an ablation stake and sonic ranger, and with a physically-based energy balance model. Universidad glacier is characterized by extremely high melt rates over the ablation season which may exceed 10 m water equivalent on the lower ablation area, representing a contribution between 10% and 13% of the total runoff observed in the upper Tinguiririca basin during the November 2009 to March 2010 period.  This contribution rises to a maximum of 34% in late summer demonstrating the importance of glacier runoff to river flow, particularly in dry summers such as 2009-2010. The temperature-index approach benefits from the availability of on-glacier meteorological data and is suited to high melt regimes, but would not be easily applicable to glaciers further north in Chile where sublimation is more significant.

## 1 Introduction

The central region of Chile (30° - 37° S), in southern South America, is characterized by a high dependence on the water supply coming from the Andes. This region, incorporating the capital city, Santiago, has more than 10 million inhabitants representing 60% of the country's population. In addition to domestic supply, water is a crucial resource for agriculture irrigation, industries, mining, hydropower generation, tourism and transport (Aitken et al., 2016; Masiokas et al., 2006; Meza et al., 2013; Ayala et al., 2016, Valdés-Pineda et al., 2014). Growing population and urban expansion in recent years is increasing the demographic pressure on water resources. In this region, winter precipitation is driven by the interactions between the westerlies circulation and the Andean natural barrier, and summer runoff is strongly influenced by the storage and release from glaciers and snow covers (Garreaud, 2013). Accurate knowledge of the processes involved in the runoff generation from mountainous areas is vital to understand and predict the availability of water resources and contribution to sea level rise (Mernild et al., 2016) especially considering the ongoing and projected future decrease in glacier volume under climate warming scenarios (Pellicciotti et al., 2014, Ragettli et al., 2016).

In these latitudes, the Andes present several peaks over 6000 m above sea level (asl) and have a mean elevation of ~4000 m asl (Garreaud, 2013). The majority of annual precipitation occurs during the winter months, which is accumulated as snow above the winter 0°C isotherm altitude, between 1500 and 3500 m asl (Garreaud, 2013). This seasonal snowpack provides an important water reservoir for the following summer months, when warm temperatures and incoming solar energy cause the melting of snow. As a consequence, rivers in the high Andes basins of central Chile are mainly driven by the melting of the seasonal snowpack (Cortés et al., 2011). However, another key source of water in the summer dry season is related to the presence of glaciers along the Andes cordillera. Crucially, glacier melt is an important source of water for Andean rivers in dry summers when little or no precipitation occurs at the upper watersheds and the seasonal snowpack is exhausted (Masiokas et al., 2013, Gascoin et al., 2010, Ohlanders et al., 2013). Peña and Nazarala (1987) estimated that the contribution of ice melt to the high basin of the Maipo River (5000 km$^2$, outlet at 850 m asl) in summer 1981/1982 was highest in February and represented 34% of total discharge.

There have been only a few physically-based distributed glacio-hydrological modelling investigations in the Andes of Chile (Pellicciotti et al., 2014; Ayala et al., 2016), which is an important limitation on understanding of current future glacier contribution to river flows, considering the current status of glacier shrinkage (e.g. Bown et al., 2008; Le Quesne et al., 2009; Malmros et al., 2016) and negative mass balance (Mernild et al., 2015) in the region. One of the most studied glaciers in the region is Juncal Norte glacier, where Pellicciotti et al. (2008) investigated the point scale energy balance and melt regime using an automatic weather station (AWS) located in the glacier ablation zone, showing that the ablation process is dominated by incoming shortwave radiation. Using a physically-based distributed glacier-hydrological model, Ragettli and Pelicciotti (2012) estimated that melted glacier ice from Juncal Norte glacier contributed 14% of the basin (241 km$^2$, 14% glacierized, outlet at ~2250 m asl) runoff for the entire hydrological year 2005/2006, with a maximum of 47% over the late ablation season (February to April). Despite these advances, results are limited to one basin and cannot necessarily be extrapolated, particularly along climatic gradients to the north and south. Other glacier energy balance studies in Chile north of 40°S have focused on improving understanding of energy fluxes and ablation at the point scale (Corripio and Purves, 2004; MacDonnell et al., 2013) or on the impact of volcanic ash on energy balance and melt (Brock et al., 2007; Rivera et al., 2008). There is therefore a lack of knowledge of spatial and temporal melt patterns at the glacier-wide scale and the progress of glacier melt contribution to downstream runoff over a full ablation season.

To address some of these issues, we present an analysis of meteorological conditions and melt for Universidad glacier, a large valley glacier in central Chile, located in a climatic transition zone with a Mediterranean climate type, between the humid temperate south and arid north of the country. The main aims are: (1) to identify the principal meteorological drivers, and surface controls, on ablation and their patterns and trends across a full ablation season; (2) to compare methods of ablation estimation using two models of differing complexity and input data requirements; and (3) to estimate the contribution of glacier melt to downstream river flows and its water resource implications. The aims are addressed using point energy balance and distributed temperature-index models forced with data from two AWS located on the glacier ablation and accumulation zones, and stream gauging records both proximal to the glacier snout and 50 km downstream at mid-altitude on the Tinguirirca river.

## 1.1 Study area

Universidad glacier (34° 40' S, 70°20' W) is located in Central Chile, in the upper part of Tinguiririca basin (1436 km$^2$), 55 km east of San Fernando city and 120 km south-east of Santiago (see Fig. 1 for location). The upper Tinguiririca basin is defined as a snowmelt dominated river (Cortez et al., 2011) with runoff peak occurring between November to January (Valdés-Pineda et al., 2014). The area of the glacier is 29.2 km$^2$ with a length of 10.6 km and an altitudinal range of 2463 m asl to 4543 m asl (Le

Quesne et al., 2009). The glacier has an accumulation zone divided in two basins which converge at an altitude of ~2900 m asl. Below this elevation, the glacier has a well-defined lower tongue. The Equilibrium Line Altitude (ELA) for the 2009-2010 hydrologic year, based on the position of the end of summer snowline was located in the range between 3500 and 3700 m asl depending the aspect of the glacier (Fig. 1). The general aspect is southerly, but the west accumulation zone has an easterly aspect. Universidad is a valley glacier that is part of a more extended glacier complex, which includes the Cipreses glacier flowing to the north, Palomo glacier flowing to the north-east, Cortaderal glacier flowing to the east, and other small glaciers flowing to the west. Another feature of the basin is the presence of small lakes mainly associated with glaciers (proglacial lakes) and debris-covered glaciers (supraglacial lakes).

Scientific investigations at Universidad glacier were initiated by Lliboutry (1958) who described some morphological characteristics of the glacier surface including ogives, blue bands, penitents and moraines. A frontal retreat of 1000 m for the period 1955-2007 was documented from aerial photographs, historical documents, tree ring chronologies and satellite images (Le Quesne et al., 2009). More recently Wilson et al. (2016) estimated Universidad glacier surface velocities between 1967 and 2015. This analysis reveals an increase in the surface velocities between 1967 and 1987, followed by a deceleration between 1987 and 2015. Also a cumulative retreat of 465 ± 44 m was found between 1967 and 2015.

## 2 Data and methods

### 2.1 Experimental setting

The study focuses on the ablation season (1 October to 31 March) of the 2009/2010 hydrological year, when the discharge, meteorological and glaciological conditions were monitored. We focused on one ablation season due to availability of data (after March 2010 no more data/observations were obtained from the glacier). The 2009/2010 hydrological year is of significance as it marks the beginning of a period of extreme aridity (2010-2015) in central and southern Chile (Bosier et al., 2016).
Data collected include meteorological observations at two AWS, surface lowering monitoring from ablation stakes and a sonic ranger (Fig. 1), satellite-derived snow cover distribution and discharge measurements in the proglacial stream. After the analysis of energy fluxes at the location of the lower AWS, a temperature-index model was calibrated and applied at the glacier scale. Resulting melt amounts were used to estimate total glacier discharge, which is compared with downstream discharge records.

### 2.2 Automatic weather stations (AWS)

Two AWS were installed on the surface of the glacier (Fig. 1). One was installed in the ablation zone (AWS1, 34° 42' S, 70° 20' W, 2650 m asl) and the second one was installed in the accumulation zone (AWS2, 34° 38′ S, 70°19' W, 3626 m asl). AWS1 recorded full energy balance variables including air temperature, humidity, wind speed and direction, net all-wave radiation, incoming shortwave radiation and atmospheric pressure, while AWS2 recorded the same variables but omitting radiation measurements. Although AWS1 was installed at the beginning of 2009 we restricted the analysis to the ablation season defined as 1 October 2009 to 31 March 2010. AWS2 recorded data from 10 December 2009 to 31 March 2010. Both AWS recorded data averaged at a 15 minute interval; however, we use hourly mean values as model inputs.

### 2.3 Ablation measurements: stakes and sonic ranger

Three stakes installed in the ablation zone of the glacier between 30 September and 3 October 2009 were read on 21 November while the surface was still snow covered at each stake (Fig. 1, Table 1). Stake 1 was located close to AWS1 and was used to assess point melt estimations from the different models. Snow density was measured using the standard Mount Rose procedure

(U.S. Department of Agriculture, 1959) on the days of installation and re-measurement of stakes. We calculated the mean snow density (Table 1) and water equivalent (w.e.) surface ablation for each stake.

A Campbell Scientific SR-50 sonic ranging sensor was installed next to AWS1. The sensor recorded surface lowering continuously every 15 minutes during a 73 day period. SR-50 data were filtered using a Hampel filter (Pearson, 2002) and then hourly means were calculated. Lowering measurements were converted to w.e. ablation values using snow density measured at stakes (Table 1).

## 2.4 Snowline elevation estimation using MODIS snow product

We used the MODIS/Terra L3 global daily snow cover product (MOD10A1, Hall et al., 2002) with a spatial resolution of 500 m which retrieves subpixel fractional snow cover area. MOD10A1 was developed using regression with Landsat TM (30 m spatial resolution) Normalized Difference Snow Index (NDSI), offering a much more accurate approach for detecting snow covered area than previous satellite snow-cover products (Cortés et al., 2014). In order to map the snow line throughout the monitored period, we obtained the hypsometric curve of Tinguiririca basin from an ASTER GDEM V2 (Tachikawa et al., 2011) and then calculated the snowline altitude for the austral summer of 2009-2010 in the upper Tinguiririca basin. The MODIS snow cover product was used only if the cloud fraction for each satellite image was less than 30%. The snowline altitude on days of high cloud cover was estimated using a linear interpolation between the last day before and the first day after the data gap. The time series of snowline altitude is used as an input for modelling to define snow or ice surface areas on the glacier. We have used the MOD10A1 product since it provides a reliable differentiation of the ice surface of Universidad glacier, which is dirty due the presence of ogives, debris and impurities, from the fresh snow areas. However, the MOD10A1 product gives the fractional snow cover for each pixel in the range 0 to 100, and to assure a correct snowline altitude we assumed the presence of snow in the pixel only when the fractional value was 100. Despite this we expect some uncertainties in the snowline altitude

## 2.5 Degree-hour model (DHM)

We applied a standard degree-day model (DDM) (e.g. Hock, 2003, 2005) at an hourly time step, in order to estimate glacier surface melt during the 2009/2010 ablation season. The model was forced with hourly temperature data from AWS1.

Melt is calculated by multiplying the hourly positive temperature, $T_h^+$ by a factor that relates temperature and melt, which we refer to as the degree-day factor ($F_{DD}$), or degree-hour factor ($F_{DH}$) when applied at an hourly interval (De Michele et al., 2013). We use stake 1 ablation measurements (Table 1) and the mean positive air temperature (4.6 °C) at AWS1 to estimate a $F_{DH}$ for snow. The percentage of hours with positive temperatures was close to 75%, therefore we used only time steps with positive values. Dividing the ablation value by the mean of positive air temperature (Braithwaite et al., 1998), we obtained a $F_{DH}$ for snow of 0.12 mm w.e. °C$^{-1}$ h$^{-1}$. The $F_{DH}$ is multiplied by the positive hourly temperature at hourly interval and results are summed for every day. As we did not have ablation stake measurements in the period when the ice surface is exposed, we used a range of published $F_{DD}$ (Hock, 2003) to obtain a range of uncertainty in calculated melt. In this case we used values between 7 and 9 mm w.e. °C$^{-1}$ d$^{-1}$, commonly used for glacier ice. The hourly $F_{DH}$ for ice was calculated by dividing the ice $F_{DD}$ by 24 to give $F_{DH}$ for ice of 0.29 and 0.38 mm w.e. °C$^{-1}$ h$^{-1}$, respectively.

Therefore melt, $a$ (mm w.e. h$^{-1}$), is estimated by the following relationship:

$$a(t,z) = F_{DH} T_h^+(t,z), \tag{1}$$

The published $F_{DD}$ values for ice were calibrated for daily average temperature and therefore could lead to a melt overestimation when applied as $F_{DH}$s in the hourly model, since calculations are only made for hours with positive temperature. To test this

potential bias, we compared melt calculations between a standard degree-day model and the DHM, using a $F_{DD}$ of 9 mm w.e. °C$^{-1}$ d$^{-1}$ and $F_{DH}$ of 0.38 mm °C$^{-1}$ h$^{-1}$, for the period of ice exposure at AWS1 and AWS2, representing the ablation and accumulation zones, respectively.  At AWS1, the difference between daily and hourly model results is negligible (<2 mm w.e. out of a total of >8000 mm w.e.). This small difference reflects the more or less continuous positive temperature in the lower ablation zone during the study period (Fig. 2). At AWS2, the DHM overestimation is more significant at 290 mm w.e. out of a total of ~2000 mm w.e., representing an increase in melt of 15% over the DDM. This is due to more frequent negative temperatures in the accumulation zone during summer months. Melt overestimation in the accumulation zone will have a small impact on total glacier runoff, which is dominated by melt from the ablation zone. Furthermore, there will be no melt estimation bias on snow as the $F_{DH}$ for snow was calibrated using measurements from Universidad glacier. We therefore apply the DHM in our calculations as it has the advantage of enabling hourly variations in temperature lapse rate to be accounted for in the distributed melt calculations across the glacier (next section).

## 2.6 Distributed degree-hour model (DDHM)

To distribute the DHM (distributed DHM, DDHM hereafter) we calculated the temperature lapse rate (LR) using both AWS in the common period (Fig. 2). Following the recommendation of Petersen and Pellicciotti (2011), we estimated a daily LR cycle considering that melt occurs mostly during the day. The mean hourly temperature gradient over an average day oscillates between -0.004 °C m$^{-1}$ to -0.007 °C m$^{-1}$. During the night (24:00 to 08:00 local time) the mean temperature gradient was close to -0.006 °C m$^{-1}$ and fairly constant.  During the day the LR has two cycles with minima in magnitude close to -0.005 °C m$^{-1}$ at 11:00 and -0.004°C m$^{-1}$ at 19:00, separated by a maximum of -0.007 °C m$^{-1}$ at 16:00. The LR minima are likely to be related to the strengthening of katabatic flow during the daytime (Petersen and Pellicciotti, 2011) and the afternoon maximum potentially due to the erosion of the katabatic boundary layer on the lower glacier tongue and warm air advected from bare rock surfaces at the glacier sides and proglacial area (van de Broeke, 1997; Ayala et al., 2015).

Using the hourly LR, we distributed the air temperatures over the entire glacier surface on a 30 m grid at an hourly time step, using the ASTER GDEM V2 and the glacier outline which was digitized from an ASTER image of 27 March, 2010. For October and November we assumed the same hourly lapse rate observed in the common period (December to March). Calculated melt values were not adjusted for reduction under debris cover on a medial moraine in the ablation zone.

## 2.7 Energy balance model (EBM)

A point scale energy balance model (EBM hereafter) was applied using weather station data collected at the AWS1, between 1 October 2009 and 29 January, 2010. We restrict use of data only up until this date because a sharp change in net radiation and incoming shortwave radiation occurs after 29th January, therefore data from late January onwards are of questionable accuracy.

Energy available for ablation, $\psi$ (W m$^{-2}$) was determined following Oerlemans (2010):

$$\psi = S_{in} + S_{ref} + L_{in} + L_{out} + H_s + H_l, \tag{2}$$

Where $S_{in}$ and $S_{ref}$ are incoming and reflected solar shortwave radiation, $L_{in}$ and $L_{out}$ are incoming and outgoing longwave radiation and $H_s$ and $H_l$ are the turbulent fluxes of sensible and latent heat, respectively. In this study, the conductive heat flux is considered negligible due to the predominantly positive air temperatures (Fig. 2) and, as precipitation totals are small in summer in the study region, the amount of sensible heat brought to the surface by rain or snow is neglected (e.g. Oerlemans and Klok, 2002). The balance of the radiative fluxes $S_{in}$, $S_{ref}$, $L_{in}$ and $L_{out}$ were directly measured by the net radiometer sensor of the AWS1. The sensible heat fluxes were calculated using the bulk approach (Cuffey and Paterson, 2010):

$$H_s = \rho_a c_a C^* u [T - T_s] \; (\Phi_m \Phi_h)^{-1}, \tag{3}$$

$u$ is wind speed in m s$^{-1}$, $T$ is air temperature in $K$ and $T_s$ ice surface temperature which is assumed to be a constant of 273.15 K (0°C). $C^*$ is a dimensionless transfer coefficient, which is a function of the surface aerodynamic roughness ($z_o$), assumed to be 0.001 m for melting snow and 0.01 m for ice on mid latitude glaciers (Brock et al., 2006):

$$C^* = \frac{k_0^2}{\ln^2 \left(\frac{z}{z_o}\right)}, \tag{4}$$

$z$ is the height above the surface of the $T$ and $u$ measurements (2 m) and $k$ is the von Kárman's constant (0.4). $\rho_a$ is the density of air which depends on atmospheric pressure $P$ in Pa:

$$\rho_a = \rho_a^o \frac{P}{P_0}, \tag{5}$$

Where $\rho_a^o$ (1.29 kg m$^{-3}$) is the density at standard pressure $P_0$ (101300 Pa). Finally $c_a$ is the specific heat of air at a constant
10   pressure (J kg$^{-1}$ K$^{-1}$) calculated as (Brock and Arnold, 2000):

$$c_a = 1004.67 \left( 1 + 0.84 \left( 0.622 \left( \frac{e}{P} \right) \right) \right), \tag{6}$$

The latent heat flux $H_l$ is:

$$H_l = \frac{0.622 \, \rho_a \, L_{v/s} C^* u [e - e_s]}{P} (\Phi_m \Phi_h)^{-1}, \tag{7}$$

$e$ is vapour pressure above the surface, $e_s$ is the vapour pressure at the glacier surface which is assumed to be 611 Pa (Brock &
15   Arnold, 2000) the vapour pressure of a melting surface, $L_{v/s}$ is the latent heat of vaporization or sublimation, depending on whether the surface temperature is at melting point (0°C) or below melting point (<0°C), respectively. Due to the absence of snow temperature measurements, the air temperature is assumed to determine the condition of evaporation or sublimation over the surface.

$e$ is obtained from the observed relative humidity at AWS1 ($f$) and using the empirical formula of Clausius-Clapeyron (Bolton,
20   1980), which is only function of air temperature ($T$ in °C):

$$e_{sat}(T) = 6.112 \exp \left( \frac{17.67 \, T}{T + 243.5} \right), \tag{8}$$

And $e$ is found by rearranging the following equation:

$$f = 100 \left( \frac{e}{e_{sat}} \right), \tag{9}$$

Melt rate ($M$) is calculated following (Hock, 2005):

$$M = \frac{\psi}{L_m \rho_w}, \tag{10}$$

$L_m$ is the latent heat of fusion and $\rho_w$ is the water density (1000 kg m$^{-3}$). Sublimation rate ($S$) is calculated (Cuffey and Paterson, 2010):

$$S = \frac{H_l}{L_s \rho_w}, \tag{11}$$

$L_s$ is the latent heat of sublimation.

Stability corrections were applied to turbulent fluxes using the bulk Richardson number ($Ri_b$), which is used to describe the stability of the surface layer (Oke, 1987):

for $Ri_b$ positive (stable): $(\Phi_m \Phi_h)^{-1} = (\Phi_m \Phi_v)^{-1}$

$$= (1 - 5Ri_b)^2, \tag{12}$$

for $Ri_b$ negative (unstable): $(\Phi_m \Phi_h)^{-1} = (\Phi_m \Phi_v)^{-1}$

$$= (1 - 16Ri_b)^{0.75}.$$

$Ri_b$ is used to describe the stability of the surface layer:

$$Ri_b = \frac{g(T-T_s)(z-z_0)}{Tu^2}, \tag{13}$$

Where $g$ is the acceleration due to gravity, $z$ is the height of the meteorological observation (2 m).

## 2.8 Proglacial discharge estimation

The estimation of the river discharge was based on the determination of the cross section geometry and the monitoring of water level in the proglacial stream. Water level in the stream was monitored using a submersible pressure transducer (KPSI Series 500), installed 500 meters downstream of the glacier terminus (2428 m asl), which registered hourly water levels from 24 November 24 2009, until 14 April 2010. The proglacial stream receives the waters draining from an 86 km² catchment, partially covered by the Universidad glacier (29.2 km²) and some debris-covered ice bodies (4.4 km²) (DGA, 2011).

In order to convert automatic water level measurements into discharge, we applied the widely used Manning's equation (Phillips and Tadayon, 2006; Fang et al., 2010; Gascoin et al., 2010; Finger et al., 2011) which combines environmental parameters such as stream slope, bed roughness and river section shape and area, for uniform open channel flow. It defines the discharge $Q$ [m³ s$^{-1}$] as follows:

$$Q = VA, \tag{14}$$

Where $A$ is the area of the cross section and $V$ is the average instantaneous velocity in the channel which is defined as:

$$V = \frac{1}{n} R^{\frac{2}{3}} \alpha^{\frac{1}{2}}, \tag{15}$$

Where $R$ is the hydraulic radius, $\alpha$ is the slope of water surface, and $n$ is the Manning coefficient of roughness.

The geometry of the channel cross section were measured in the field at the location of the pressure transducer. The hydraulic radius is a measure of channel flow efficiency and is defined as the ratio of the cross sectional area to its wetted perimeter. We used the ASTER GDEM of 30 m to estimate the slope of the terrain in the gauged section. The roughness coefficient was set as 0.05, according to the United States Geological Survey (USGS) value for cobble and boulder bedrocks (Phillips and Tadayon, 2006), which correspond to our site. The area of the cross section $A$ was estimated using water level observations from the pressure transducer and the width of the wet section, which in turn is estimated from an empirical relationship with water level.

We also make use of two other streamflow gauge measurements (see Fig. 1). The first is operated by a private company, Pacific HydroChile, located 1700 m from the glacier snout recording data every hour. The second one is operated by the Dirección General de Aguas (DGA), and is located on Tinguiririca river at 560 m asl, 50 km downstream the Universidad glacier. The contributing watershed to this lower gauge has an area of 1436 km² with a total ice cover of 81 km² (DGA, 2011), among which Universidad glacier is by far the largest single ice body.

### 2.9 Discharge routing

Estimated glacier melt obtained with the DDHM for each 30 m grid cell and each time step was transformed into discharge using a linear reservoir model (Baker et al., 1982; Hock and Noetzli, 1997). For hourly time intervals, the proglacial discharge $Q$ is given by:

$$Q(t_2) = Q(t_1)e^{-1/k} + M(t_2) - M(t_2)e^{-1/k}, \qquad (16)$$

Where $M(t)$ is the rate of water inflow to the reservoir, which is considered to be equivalent to the total glacier melt. $k$ is the factor of proportionality in hours and is estimated from the time it takes for the water entering the top of the reservoir to flow out of the bottom (Baker et al., 1982).

## 3 Results

### 3.1 Meteorological and snow conditions for the ablation period (October 2009 to March 2010)

Time series of meteorological variables are shown in Fig. 2. At AWS1 temperature is generally above 0°C during December-March even during the night, while temperature at AWS2 shows more frequent negative values during the night (Fig. 2). Wind speed shows some inter-daily variability but the hourly values are predominantly between 2 and 8 m s$^{-1}$. Wind speed was generally lower in summer (December to March) than spring (October to November). The prevailing wind direction (~10° to
15 ~45°) corresponds to the general ice flow direction (Fig. 4), indicating a strong and persistent katabatic wind. The daily cycle of wind direction reveals that predominant katabatic wind is slightly weakened during afternoon hours (between 14:00 to 18:00, local time, Fig. 4). Relative humidity shows a large diurnal variability. Saturation is reached during several days in the period. The snow line altitude derived from MODIS data is shown in Fig. 5. At the beginning of the ablation season the entire glacier surface was covered by snow. The snowline altitude increased gradually until mid-January and thereafter stabilized between
20 3800 and 4000 m asl. There is some variability in the snow line positioning, probably due to varying proportions of cloud cover on different days. This altitude range is slightly higher than the altitude of the ELA estimated with the ASTER image from the end of March of 2010 (Fig. 1). In the first half of the ablation season high cloud cover (greater than 30%) affected snowline detection.

### 3.2 Point scale ablation comparison: observation and modelling

25 Sonic ranger measurements and stake observations (Fig. 1) were compared to the melt estimated with the EBM and DHM at the point scale for the location of AWS1 (Fig. 6). Sublimation represents a small percentage (2.8%) of the total ablation calculated with the energy balance indicating the dominance of positive temperature and hence melt regime. Snow disappears at this location (~ 2650 m asl) near 7 November 2009.

Melt simulations from the DHM and EBM agreed well with the stake and sonic ranger ablation measurements. The DHM tended
30 to lag behind the EBM and sonic ranger until 21 November, after which the EBM and sonic ranger estimates fall within the DHM range for $F_{DH}$ between 0.29 and 0.38 mm w.e. h$^{-1}$ °C$^{-1}$. The DHM estimated little or no melt during cold periods, e.g. the first 10 days of November, whereas the EBM indicates melt (as does the sonic ranger) caused by high insolation. During warm periods, e.g. 11-16 November, the DHM estimated higher melt rates than the sonic range sensor, indicating the high sensitivity of the DHM to temperature fluctuations. At the end of the comparison series, the EBM and sonic ranger total melt are in the range
35 of the melt estimated by the DHM. Overall, despite uncertainties in snow density and melt model parameters, the good agreement between the different models and measurements, supports the use of the DDHM to estimate total glacier melt.

### 3.3 Energy balance

Figure 7 shows the daily mean of observed energy fluxes (net radiation and incoming shortwave radiation), turbulent fluxes calculated by the EBM (latent and sensible heat) and the resulting energy available for melt at AWS1, also calculated by the model. Daily mean melt energy closely matches daily mean net radiation through much of the ablation season due to compensation between generally positive $H_s$ and mainly negative $H_l$, except during warm periods such as late January when $H_l$ turns positive (Fig. 7, Table 2). Incoming shortwave radiation was the main source of melt energy (Table 2). Energy available for melt is higher in December and January and tends to diminish during February to March, in close association with the annual cycle of incoming shortwave radiation.

### 3.4 Distributed degree hour model (DDHM)

Figure 8 shows the accumulated melt for each pixel of Universidad glacier estimated by the DDHM during the period 1 October 2009 to 31 March 2010 using ice $F_{DH}$s of 0.29 and 0.38 mm h$^{-1}$ °C$^{-1}$. As the degree-hour melt is only a function of temperature, the higher zones of the glacier presented the lowest melt and *vice versa*. The maximum values of ~11000 mm w.e. (for $F_{DH}$ = 0.38 mm h$^{-1}$ °C$^{-1}$) were located on the lower glacier tongue (Fig. 9). All parts of the glacier experienced at least some melting, with melting values around 1 m w.e. in the upper accumulation area. Bare ice surfaces accounted for ~85% of the total melt.

### 3.5 Discharge

During the study period we estimated an average stream flow of 12 m³ s$^{-1}$ with a range from 4 m³ s$^{-1}$ and 43 m³ s$^{-1}$ (Fig. 10). Discharge values increased gradually between the end of November and the end of December. The mid ablation season (January and February) experienced two major discharge peaks. Subsequently, values decreased from late February to the end of March to values similar to the end of October (Fig. 10).

The hourly mean hydrographs have strong diurnal amplitude cycles (Fig.11) during the high discharge months and exhibit a characteristic shape for a glaciated catchment, with a steep rise and gradual decline (Nolin et al., 2010; Willis, 2011). Discharge peaked typically at 16:00 PM, from a minimum at 10:00 AM which, considering the large size of the glacier, indicates an efficiently channelized drainage system flow.

Water discharge estimated at the HydroChile station showed high correlation with estimations made from the water level/pressure sensor installed near the glacier front at hourly scale (r =0.92). Generally, the HydroChile station values exceeded water discharges estimated from the water pressure sensor before mid-January; thereafter the water pressure sensor derived values exceeded the HydroChile results, until 27 February when there was a large earthquake in central Chile. The sudden jump in HydroChile values around this date (Fig. 10) is likely due to this earthquake, whereas the pressure sensor derived values were adjusted for the change in water height. For comparison purposes we reject data from the HydroChile station after the earthquake.

### 3.6 Comparison of glacier melt water with total proglacial river discharge

Total glacier melt calculated with the DDHM is compared with the discharge records estimated from the pressure sensor and the gauging records from HydroChile station, at 500 m and 1700 m from the glacier snout, respectively, between 24 November, 2009 and 31 March 2010 (Figs. 1 and 12). At hourly time step, glacier melt and proglacial discharge estimations have correlations of 0.72 (pressure sensor station) and 0.75 (HydroChile station). Melt estimated from the glacier represents between the 50% and 66% of the runoff estimated from the pressure sensor, depending on the ice $F_{DH}$ value used (Fig. 12). The remaining 34% to 50% of proglacial runoff is attributed to contributions from glaciers and lakes in lateral valleys, which also contribute to

proglacial river discharge, but are not accounted for in the DDHM calculations. Moreover, during the first half of the season, the proglacial river includes snow melt runoff from the non-glaciated area of the valley.

Mean total melt from Universidad glacier represents between 10% and 13% (depending on ice $F_{DH}$ used) of the total runoff of the entire upper Tinguiririca basin (1478 km$^2$) over the November 2009 to March 2010 period (Fig. 13, DGA station, Table 3). This percentage is much more than the area of the Universidad glacier (~2%) with respect to the total basin area of the upper Tinguiririca. The percentage of glacier contribution is variable during the season (Table 3). At the beginning of the common period of pressure sensor and AWS1 measurements (end of November) runoff is dominated by the snow melt in the entire high Tinguirirca basin, reflected in the high daily variability in runoff in the DGA station until January, due the control of air temperature over snow melt (Fig. 13). In these months, the glacier melt contribution ranged between 3% and 10%. After the peak in the runoff at the end of January, the contribution of Universidad glacier to total basin runoff increased to 14-19% with peaks up to~34%.

The daily variability of all stream gauging series was similar between December and January. The DGA station measurements mainly show the additional influence of the air temperature variations on snow melt across the catchment, since the rainfall in the period of Fig. 13 was 0 mm. In February and March the DDHM calculated melt and the DGA station runoff display similar temporal variations with one to two days of lag between each.

# 4 Discussion

## 4.1 Modelling approach and uncertainties

Our results suggest that a simple empirical melt model (DDHM) is suitable for estimating glacier melt contribution to river runoff from glaciers in Chile. This interpretation is based on the close correlation between ablation estimates from the DHM and melt estimates from an energy balance model, ablation stake and sonic ranging sensor data at a point scale, and agreement between estimates of total glacier runoff and discharge estimations in the proglacial stream. This good agreement results from: first, the availability of on-glacier meteorological data; second, a locally calibrated degree-hour factor for snow; and third, an hourly-calibrated lapse rate at the glacier for spatial extrapolation of air temperature inputs to the distributed melt model. Forcing temperature-index models with off-glacier data is problematic due to the depression of near-surface air temperature within the glacier boundary layer (Shea and Moore, 2010) under positive ambient temperature conditions and variability in the strength and thickness of the katabatic boundary layer which can lead to high hourly variability in local air temperature lapse rate (Petersen and Pellicciotti, 2011; Petersen et al., 2013; Ayala et al., 2015).

The key sources of model uncertainty are: (a) snow density, which is required to convert stake and ultrasonic sensor measurements of snow into w.e. melt for model validation and calculation of degree-hour factors. Here snow density was measured only two times in the early ablation period; (b) parameters in the energy balance model: albedo was not measured but was not needed here as net all wave radiation was measured directly at AWS1; however, lack of albedo measurements prevented the application of an Enhanced temperature-index (ETI) model (Pellicciotti et al., 2008) at the glacier-wide scale; and, although the $z_0$ value cannot be evaluated due to lack of independent measurements, the small contribution of the turbulent fluxes to total melt means $z_0$ errors would account for only a small amount of total EBM error; (c) sublimation in the DDHM was ignored, but Universidad glacier has an ablation regime dominated by melt, more typical of temperate glaciers further south in Chile (Brock et al., 2007) therefore this is likely to have led to only a small overestimate of glacier runoff; (d) groundwater flows are not known and evaporative losses from glacier melt water were also unknown but considered negligible and (e) the date of ASTER GDEM is not know which could produce error in temperature distribution due to elevation changes in the glacier surface.

During periods of low positive temperature and high insolation, the DHM underestimated melt, and *vice versa* during periods of high temperature. This implies spatial and temporal errors, i.e. overestimation of melt during warm weather and on the lower glacier, and melt underestimation during cold weather and on the upper glacier, will tend to compensate over time and in summation of total glacier melt, but will lead to short term errors.

## 4.2 Glacier contribution to basin runoff

The finding that Universidad glacier, while accounting for just 2% of the total basin area, contributed between 3% and 34% of total runoff from the entire upper Tinguiririca basin over the December to March period, demonstrates the importance of glaciers for river flows in central Chile during the summer months. The overall glacier melt contribution to the Tinguiririca river would be much larger considering that the total glacier area of the basin is 81 km$^2$, representing 5.5% of the total basin area. Crucially, the glacier contribution becomes more significant over the course of the summer as other sources, principally the seasonal snowpack, become depleted. Hence, glacier runoff becomes critical to maintaining flows in the Tinguiririca river during years when summer drought extends into autumn, e.g. in the period 2010-2015 (Bosier et al., 2016), and in dry winters when snowpack accumulation at high-elevation sites is small. Research by Gascoin et al. (2011) and Pourrier et al. (2014) on glaciers of the arid Andes has revealed the hydrological importance of glaciers to the north of Tinguiriricabasin.

The recent and ongoing retreat for Universidad glacier in response to atmospheric warming (Le Quesne et al., 2009; Wilson et al., 2016) and the relevance of glacier melt contribution highlighted in this work, implies that impacts on river runoff are expected over the next decades. In the 1950-2007 period positive trend in runoff for upper Tinguiririca basin was observed (0.3 m$^3$ s$^{-1}$ y$^{-1}$, not significant) (Casassa et al., 2009). Considering that the estimated upward migration (200 m) of the zero degree isotherm between 1975-2001 in central Chile, (Carrasco et al., 2005) far exceeds the elevational retreat (~60-70 m) of the Universidad glacier snout (Wilson et al., 2016) over a longer period (1967-2015) the contributing melt area, and hence total glacier melt of Universidad glacier has increased in the last ~30 years. This increase in glacier melt might explain the positive trends in rivers of central Chile as suggested by Casassa et al. (2009). Another characteristic to consider is that the date marking the timing of the center of mass of annual flow for the upper Tinguirica shows a negative trend in the period 1961-2007 (Cortez et al., 2011), indicating the bulk of the annual flow is shifting towards earlier in the year. This implies that snowmelt tends to occurs earlier and hence glacier ice is also exposed earlier in the year, increasing the hydrological importance of glaciers.

From our analyses is uncertain wheter Tinguiririca runoff has already reached the "peak water" expected for glacierized basins as a consequence of deglaciation (Casassa et al., 2009). The observed positive recent trend in the runoff of the Tinguiririca (Masiokas et al., 2006 and Casassa et al., 2009) suggests that peak water is yet to occurs. In contrast recent modelling work has shown that peak water has already passed for e.g. the Juncal basin further to the north and that future runoff for this basin is likely to sharply decrease (Ragettli et al., 2016). Estimation of the future runoff trend and melt contribution from Universidad glacier are beyond the scope of this work, however the possibility of increased persistence and recurrence of droughts in central Chile (Boisier et al., 2016) would increase the hydrological importance of Universidad glacier in the future.

## 4.3 Comparison to other studies in Chile

According to the classification of Sagredo and Lowell (2012), Universidad glacier is located in a climatic zone, characterized by positive mean air temperature in the ablation season, which favours the summer melting. It has been shown that in high altitude glaciers of northern Chile and in the dry season of the outer tropics of Perú and Bolivia, melt rates are reduced as more ablation occurs through sublimation (Winkler et al., 2009; Sagredo and Lowell, 2012; MacDonell et al., 2013), whereas, to the south, lower incident shortwave radiation due to increasing latitude and cloud cover reduces available energy for melt (Brock et al.,

2007). Hence, Universidad glacier may be located in a climatic zone which maximizes relative summer melting. Local factor such as the large accumulation area and extension of the glacier tongue to relatively low elevation also contributes to the high melt detected in the lower zone of the glacier (Fig. 8).

Modelled ablation season melt at Universidad glacier is high in comparison to Juncal Norte glacier (33°S) where maximum accumulated melt is in the order of 5000-6000 mm w.e., depending on the model applied (Pellicciotti et al., 2014). These values are near half of the estimated values obtained at the lower tongue of Universidad glacier (Figs. 8 and 9). However, melt rate distribution shows great variations depending on altitude. The melt rate at the equilibrium line of Universidad glacier (3500 - 3700 m asl; 2000 to 2500 mm w.e.) is less than the melt at the equilibrium line (~2000 m asl) of Pichillancahue glacier in Villarrica volcano further south (39°S), where Brock et al. (2007) estimated cumulative melt of 4950 and 3960 mm w.e between January and March of 2004 and 2005 respectively. However, it is worth noting that ablation below this elevation is greatly reduced on Pichillancahue glacier by an extensive cover of thick insulating tephra.

Recently Ayala et al. (2016) estimated that ice melt contribution at the outlet of glaciers Bello, Yeso (debris-free glaciers) and Piramide (debris-covered glacier) in the central Andes (~33.53°S), depends on the meteorological conditions of each year. In snow rich years, such as 2013-2014, glaciers contributed 30% of summer water runoff while in dry years such as 2014-2015 the summer contribution was 50%. This latter value is similar to the ice melt contribution recorded at the outlet of Universidad glacier, which was in the range 42% to 58% of the total discharge estimated with the pressure sensor. Considering that almost no precipitation was recorded by weather stations close to the study site, the 2009-2010 ablation season is representative of relatively dry years in central Chile, which interestingly resulted in a similar percentage melt contribution with respect to the 2014-2015 season in Bello and Yeso glaciers. As Ayala et al. (2016) suggest, melt comparison with other glaciers must made with caution, considering that melt depends of altitudinal range, glacier characteristics, differences in atmospheric conditions for each year and even differences in methodology.

At a basin scale, glacier contribution to downstream runoff in the Tinguiririca is of similar magnitude to previous results for the central Andes, e.g. Ragettli and Pellicciotti (2012) estimate that 14% of the total runoff of the Juncal River Basin (241 km$^2$, outlet at ~2250 m asl) comes from Juncal Norte glacier (9.9 km$^2$) in the hydrological year 2005/2006 with a maximum of 47% during the late ablation season. For the Maipo basin, Peña and Nazarala (1987) estimate a mean contribution from glaciers (~7.2% of the total upper Maipo basin area) of 11.8% between hydrological years 1981/1982 and 1985/1986, with maximum values during the end of each hydrological year. An important issue of the results showed by Peña and Nazarala (1987) is that there is an interannual variability in the discharge from glaciers, for example the percentage of the glacier contribution to total runoff in the Maipo in February of 1983 was just 5%, but in February of 1982 it was 34%. It has been suggested that another source of runoff during dry years at the end of the ablation season is groundwater flow (Baraer et al., 2014; Rodriguez et al., 2016) however it is difficult to estimate this contribution at Universidad glacier without direct measurements.

## 5 Conclusions

In this study, we have investigated the climatic conditions, ablation and melt water contribution to downstream river flow of Universidad glacier, located in central Chile during the 2009-2010 summer ablation season, using a distributed degree-hour melt model, driven by data from two on-glacier weather stations. The main outcomes of this work are:

- Good agreement was found between melt estimated from degree-hour and energy balance models, and ablation stake and sonic ranger records at the lower weather station site in the ablation zone, supporting the application of a simple temperature-

index method of calculating total glacier melt at this location. The degree-hour model was distributed at the glacier wide scale accounting for hourly variations in the local temperature lapse rate, which tended to be shallower during the daytime, when most melt occurs.

- The ablation regime is dominated by incoming shortwave radiation, with highest melt rates occurring during December to February, and is also characterized by high air temperature which is almost continuously positive on the lower ablation zone between November and March. These climatic conditions result in very high melt totals, which exceed 10 m w. e. melt on the lower tongue and are thus greater than melt values reported for other glaciers in central Chile. This is attributed to the relative insignificance of sublimation to total ablation, and the high insolation due to low cloud cover and latitudinal location, combined with predominantly positive air temperature. Melt totals were much lower in the accumulation area due to lower temperatures and persistent snow cover above about ~3800 m.

- By comparing total glacier melt with discharge estimates 0.5 km from the glacier snout, and discharge measurements at gauges at 1.7 km and 50 km downstream on the Tinguiririca river, we estimate that Universidad glacier, contributed between 10% and 13% of the total runoff observed in the upper Tinguiririca basin for the period November 2009 to March 2010. The total contribution of all glaciers to runoff in the upper Tinguiririca basin will be greater considering that Universidad glacier only represents 36% of the total glacier area of the basin (~81 km$^2$). During the late ablation season, in February and March 2010, when other runoff sources such as snowmelt become depleted, the daily contribution of Universidad glacier to total runoff in the Tinguiririca reached as high as 34%.

The successful application of a simple temperature-index melt model to estimate total seasonal melt at Universidad glacier is partly a consequence of the predominant high melt regime of this glacier which favors the application of the degree-hour model. In this sense, estimation of runoff contributions from glaciers in northern Chile is more challenging as an increasing proportion of ablation energy is consumed by sublimation (MacDonell et al., 2013) which cannot be estimated from simple temperature-index methods.

Climatic warming, leading to a rapid rise in the zero-degree isotherm (Carrasco et al. 2005) and upward expansion of glacier melt contributing area into the accumulation zone, means Universidad glacier will continue to make a crucial, and perhaps an increasing, contribution to downstream flows in the next few decades, particularly as smaller glaciers in the basin disappear. In the long term, glacier shrinkage will lead to a depletion of glacier melt and in downstream flow in the Tinguiririca, particularly in late summer, with severe implications for human activities in the river valley such as mining, domestic consumption, industry, forestry, tourism, forestry and agriculture (Aitken et al., 2016) and irrigation and hydropower generation (Valdés-Pineda et al., 2014). The potential for hydropower generation on the Tinguiririca river has been recognized (Pelto, 2010), with plants already working at La Higuera and La Confluencia, which can be affected by interannual variability and medium to long term trends. Finally, more studies are necessary to establish the inter-annual variability of glaciers contribution for entire basins in order to help manage future water availability, considering climate change and the increasing demand for water in the region.

**Acknowledgments**

This work was supported by CECs, which is funded by the Chilean Government through the Centers of Excellence Base Financing Program of Comisión Nacional de Investigación Científica y Tecnológica de Chile (CONICYT). Pablo Zenteno and Camilo Rada assisted with data collection. The Chilean Water Cadastre (DGA) also provided data and support to this paper. We would like to thank Christophe Kinnard for sharing his data. We would like to thank to two anonymous referees for their constructive and useful comments and recommendations.

**References**

Aitken, D., Rivera, D., Godoy-Faúndez, A., Holzapfel, E.: Water Scarcity and the Impact of the Mining and Agricultural Sectors in Chile, Sustainability, 8, 1-18, 2016.

Ayala, A., Pellicciotti, F., and Shea, J.M.: Modelling 2m air temperatures over mountain glaciers: Exploring the influence of katabatic cooling and external warming, J. Geophys. Res. Atmos., 120, 1–19,doi:10.1002/2015JD023137, 2015.

Ayala, A., Pellicciotti, F., MacDonell, S., McPhee, J., Vivero, S., Campos, C., and Egli, P.: Modelling the hydrological response of debris-free and debris-covered glaciers to present climatic conditions in the semiarid Andes of central Chile, Hydrol. Process., doi: 10.1002/hyp.10971, 2016.

Baker, D., Escher-Vetter, H., Moser, H., Oerter, H., and Reinwarth, O.: A glacier discharge model based on results from field studies of energy balance, water storages and flow, International Association of Hydrological Science Publication, 138 (Symposium at Exeter 1982 – Hydrological Aspects of Alpine and High Mountain Areas), 103-112, 1982.

Baraer, M, Mckenzie, J., Mark, B. G., Gordon, R., Condom, T., Bury, J., Gomez, J., Knox, S., and Fortner, S.K.: Contribution of groundwater to the outflow from ungauged glacierized catchments: a multi-site study in the tropical Cordillera Blanca, Perú, Hydrol. Process. 29, 2561-2581, 2014.

Bolton, D.: The Computation of Equivalent Potential Temperature, Mon. Wea. Rev., 108, 1046–1053, 1980.

Bosier, J.P., Rondanelli, R., Garreaud, R., Muñoz, F.: Natural and anthropogenic contributions to the Southeast Pacific precipitation decline and recent mega-drought in central Chile, Geophys. Res. Lett., 43, 1-9, doi:10.1002/2015GL067265, 2016.

Bown, F., Rivera, A., and Acuña, C.: Recent glaciers variations at the Aconcagua basin, central Chilean Andes, Ann Glaciol., 48, 43-48, 2008.

Braithwaite, R J., Konzelmann, T., Marty, C., and Olesen O.B.: Errors in daily ablation measurements in northern Greenland, 1993-94, and their implications for glacier climate studies, J. Glaciol., 44, 583-588, 1998.

Brock, B. and Arnold, N.: A spreadsheet-based (Microsoft Excel) point surface energy balance model for glacier and snowmelt studies, Earth Surf. Proc. Land., 25, 649-658, 2000.

Brock, B.W., Willis, I.C., and Sharp, M.J.: Measurement and parameterisation of aerodynamic roughness length variations at Haut Glacier D'Arolla, Switzerland. Ann. Glaciol., 52, 281–297, 2006.

Brock, B., Rivera, A., Casassa, G., Bown, F. and Acuña C.: The surface energy balance of an active ice-covered volcano: Volcán Villarrica, southern Chile, Ann. Glaciol., 45, 104-114, 2007.

Carrasco, J., Casassa, G., and Quintana, J.: Changes of the 0°C isotherm and the equilibrium line altitude in central Chile during the last quarter of the 20th century, Hydrol. Sci. J., 50, 933–948, 2005.

Casassa, G., López, P., Pouyaud, B. and Escobar, F.: Detection of changes in glacial run-off in alpine basins: examples from North America, the Alps, central Asia and the Andes, Hydrol. Process., 23: 31–41, 2009.

Corripio, J. G. and Purves, R. S.: Surface Energy Balance of High Altitude Glaciers in the Central Andes: the Effect of Snow Penitentes, in Climate and Hydrology in Mountain Areas, edited by: de Jong, C., Collins, D., and Ranzi, R., Wiley & Sons, London.,15–27, 2004.

Cortés, G., Vargas, X., and McPhee, J.: Climatic sensitivity of streamflow timing in the extratropical western Andes Cordillera. J Hydrol., 405, 93–109, 2011.

Cortés, G., Girotto, M., and Margulis, S.: Analysis of minimum glacier and snow extent over the Andes using historical Landsat imagery, Remote Sens. Environ., 141, 64-78, 2014.

Cuffey, K. M. and Paterson, W. S. B.: The Physics of Glaciers, 4th Edn., Elsevier, Oxford, UK, 2010

De Michele, C., Avanzi, F., Ghezzi, A, and Jommi, C.: Investigating the dynamics of bulk snow density in dry and wet conditions using a one-dimensional model, The Cryosphere, 7, 433–444, 2013.

Dirección General de Aguas: Catastro, exploración y estudio de glaciares en Chile central. S.I.T. N° 265, Santiago, 2011.

Fang, X., Pomeroy, J. W., Westbrook, C. J., Guo, X., Minke, A. G., and Brown T.: Prediction of snowmelt derived streamflow in a wetland dominated prairie basin, Hydrol. Earth Syst. Sci., 14, 991–1006, 2010.

Finger, D., Pellicciotti, F., Konz, M., Rimkus, S., and Burlando, P.: The value of glacier mass balance, satellite snow cover images, and hourly discharge for improving the performance of a physically based distributed hydrological model, Water Resour.Res., 47, W07519, doi:10.1029/2010WR009824, 2011.

Garreaud, R.: Warm winter storms in Central Chile, J. Hydrometeorol., 14, 1515-1534, 2013

Gascoin, S., Kinnard, C., Ponce, R., Lhermitte, S., MacDonell, S., and Rabatel, A.: Glacier contribution to streamflow in two headwaters of the Huasco River, Dry Andes of Chile, The Cryosphere, 5, 1099–1113, 2011

Hall, D. K., Riggs, G. A., Salomonson, V. V., Di Girolamo, N. E., and Bayr, K. J.: MODIS snow cover products, Remote Sens. Environ., 83, 181–194, 2002.

Hock, R. and Ch. Noetzli,: Areal mass balance and discharge modelling of Storglaciären, Sweden, Ann. Glaciol., 24, 211-217, 1997.

Hock, R.: Temperature index melt modelling in mountain regions, J. Hydrol., 282, 104-115, 2003.

Hock, R.: Glacier melt: a review of processes and their modelling, Prog. Phys. Geog., 29, 362-391, 2005.

Le Quesne, C., Acuña, C., Boninsegna, J.A., Rivera, A., and J. Barichivich, J.: Long-term glacier variations in the Central Andes of Argentina and Chile, inferred from historical records and tree-ring reconstructed precipitation, Palaeogeogr. Palaeoc., 281, 334-344, 2009.

Lliboutry, L.: Studies of the shrinkage after a sudden advance, blue bands and wave ogives on glaciar Universidad (Central Chilean Andes), J. Glaciol., 3, 261-270, 1958.

MacDonell, S., Kinnard, C., Molg, T., Nicholson, L. and Abermann, J.: Meteorological drivers of ablation processes on a cold glacier in the semi-arid Andes of Chile, The Cryosphere, 7, 1513-1526, 2013.

Malmros, J. K., Mernild, S. H., Wilson, R., Fensholt, R., and Yde, J. C. : Glacier area changes in the central Chilean and Argentinean Andes 1955 – 2013/2014. J.Glaciol, 62, 391–401, 2016.

Masiokas, M.H., Villalba, R., Luckman, B.H., Le Quesne, C., and Aravena, J.C.: Snowpack variations in the central Andes of Argentina and Chile, 1951-2005: Large-scale atmospheric influences and implications for water resources in the region, J. Climate, 19, 6334-6352, 2006.

Masiokas, M.H., Villalba, R., Luckman, B.H., Montaña E., Betman, E., Christie, D.A., LeQuesne, C., and Mauget, S.: Recent and historic Andean snowpack and streamflow variations and vulnerability to water shortages in central-western Argentina. In: Climate Vulnerability: Understanding and Addressing Threats to Essential Resources. Elsevier Inc., Academic Press, 2013.

Mernild, S. H., Beckerman, A. P., Yde, J. C., Hanna, E., Malmros, J. K., Wilson, R., and Zemp, M.: Mass loss and imbalance of glaciers along the Andes to the sub-Antarctic islands. Global Planet. Change, 1–11, 2015.

Mernild, S. H., Liston, G. E., Hiemstra, C. A., Wilson, R.: The Andes Cordillera. Part III: Glacier Surface Mass Balance and Contribution to Sea Level Rise (1979–2014).Int. J. Climatol., doi: 10.1002/joc.4907, 2016

Meza, F.J., Wilks, D.S., Gurovich, L., and Bambach, N.: Impacts of climate change on irrigated agriculture in the Maipo basin, Chile: reliability of water rights and changes in the demand for irrigation. J. Water Res. Pl-ASCE, 139. 554-564, 2013.

Nolin A.W., Phillippe J., Jefferson A., and Lewis S.L.: Present-day and future contributions of glacier runoff to summer time flows in a Pacific Northwest watershed: Implications for water resources, Water Resour. Res., 46, W12509, doi:10.1029/2009WR008968, 2010.

Oerlemans, J. and Klok, E.J.: Energy balance of a glacier surface: analysis of Automatic Weather Station data from the Morteratschgletscher, Switzerland, Arct. Antarct. Alp. Res., 34, 477-485, 2002.

Oerlemans, J.: The microclimate of valley glaciers, Igitur, Utrecht University, Utrecht, 2010.

Ohlanders N., Rodriguez M., and McPhee J.: Stable water isotope variation in a Central Andean watershed dominated by glacier and snowmelt, Hydrol. Earth Syst. Sci., 17, 1035– 1050, 2013.

Oke, T. R.: Boundary Layer Climates. Second Edition, Routledge, 423 pp., 1987

Pelto. M.: Hydropower: Hydroelectric power generation from alpine glacier melt. in: Encyclopedia of Snow, Ice and Glaciers, edited by: Singh, V. P., Singh, P., and Haritashya, U. K., Springer, Dordrecht, the Netherlands, 546-551, 2011

Pellicciotti, F., Helbing, J., Rivera A., Favier, V., Corripio, J., Araos, J. and Sicart J.E.: A study of the energy-balance and melt regime of Juncal Norte glacier, semi-arid Andes of central Chile, using models of different complexity, Hydrol. Process, 22, 3980-3997, 2008.

Pellicciotti, F., Ragettli, S., Carenzo, M., and McPhee, J.: Changes of glaciers in the Andes of Chile and priorities for future work, Sci. Total Environ., 493, 1197-1210, 2014.

Peña, H., and Nazarala, B.: Snowmelt runoff simulation model of a central Chile Andean basin with relevant orographic effects, in: Large Scale Effects of Seasonal Snow Cover, IAHS Publ. No.166, Vancouver, Canada, 1987.

Petersen, L., and Pellicciotti, F.: Spatial and temporal variability of air temperature on a melting glacier: Atmospheric controls, extrapolation methods and their effect on melt modelling, Juncal Norte Glacier, Chile, J. Geophys. Res., 116,D23109, doi:10.1029/2011JD015842, 2011.

Petersen L., Pellicciotti F., Juszak I., Carenzo, M. and Brock B.W.: Suitability of a constant air temperature lapse rate over an Alpine glacier: testing the Greuell and Böhm model as an alternative, Ann. Glaciol., 54, 120–130, 2013.

Phillips, J., and Tadayon, S.: Selection of Manning's roughness coefficient for natural and constructed vegetated and non-vegetated channels, and vegetation maintenance plan guidelines for vegetated channels in Central Arizona. U.S. Geological Survey Scientific Investigations Report 2006-5108, 2006.

Pourrier, J., Jourde, H., Kinnard C., Gascoin S., and Monnier S.: Glacier meltwater flow paths and storage in a geomorphologically complex glacial foreland: The case of the Tapado glacier, dry Andes of Chile (30°S), J. Hydrol., 519, 1068–1083 doi: 10.1016/j.jhydrol.2014.08.023, 2014.

Ragettli, S., and Pellicciotti, F.: Calibration of a physically-based, fully distributed hydrological model in a glacierized basin: on the use of knowledge from glacio-meteorological processes to constrain model parameters, Water Resour. Res., 48, W03509, doi:10.1029/2011WR010559, 2012

Ragettli, S., Immerzeel, W., and Pellicciotti, F.: Contrasting climate change impact on river flows from high-altitude catchments in the Himalayan and Andes Mountains, P. Natl. Acad. Sci. USA, 133, 9222–92227, 2016.

Rivera, A., Corripio, J. G. Brock, B.W., Clavero, J., and Wendt, J.: Monitoring ice capped active Volcán Villarrica in Southern Chile by means of terrestrial photography combined with automatic weather stations and GPS, J. Glaciol., 54, 920 – 930, 2008.

Rodriguez, M., Ohlanders, N., Pellicciotti, F., Williams, M. W., and McPhee, J.: Estimating runoff from a glacierized catchment using natural tracers in the semi-arid Andes cordillera, Hydrol. Process., 30, 3609–3626, 2016.

Sagredo, E. and Lowell, T.: Climatology of Andean glaciers: A framework to understand glacier response to climate change, Global Planet. Change, 86–87, 101–109, 2012.

Shea, J.M. and Moore, R.D.: Prediction of spatially distributed regional-scale fields of air temperature and vapour pressure over mountain glaciers, J. Geophys. Res., 115, D23107, doi:10.1029/2010JD014351, 2010.

U.S. Department of Agriculture, Soil Conservation Service.: Snow survey sampling guide, Agriculture Handbook N°169, 33 pp, 1959.

Tachikawa, T., Kaku, M., Iwasaki, A. Gesch, D., Oimoen, M., Zhang, Z., Danielson, J., Krieger, T., Curtis, B., Hasse, J., Abrams, M., Crippen, R., and Carbajal, C.: ASTER Global Digital Elevation Model Version 2 – Summary of Validation Results http://lpdaacaster.cr.usgs.gov/GDEM/Summary_GDEM2_validation_report_final.pdf (accessed 4 December 2015), 2011.

Valdés-Pineda, R., Pizarro, R., García-Chevesich, P., Valdés, J.B., Olivares, C., Vera, M., Balocchi, F., Pérez, F., Vallejos, C., Fuentes, R., Abarza, A., and Helwig, B.: Water governance in Chile: Availability, management and climate change, J. Hydrol., 519, 2538–2567, 2014.

van den Broeke, M. R.: Momentum, heat, and moisture budgets of the katabatic wind layer over a midlatitude glacier in summer, J. Appl. Meteorol., 36, 763–774, 1997.

Willis, I.C.: Hydrographs, in Encyclopedia of Snow, Ice and Glaciers, edited by: Singh, V., Singh, P., and Haritashya, U., Springer, the Netherlands, 534–538, 2011.

Wilson, R., Mernild, S., Malmros, J., Bravo, C., and Carrión, D.: Surface velocity fluctuations for Glaciar Universidad, central Chile, between 1967 and 2015, J.Glaciol, 62, 847-860, 2016.

Winkler, M., Juen, I., Mölg, T., Wagnon, P., Gómez, J. and Kaser G.: Measured and modelled sublimation on the tropical Glaciar Artesonraju, Peru, The Cryosphere, 3, 21-30, 2009.

**Table 1: Stake ablation measurements**

| Stake N° | Altitude (m asl) | Installation date | Measurement date | Difference (m) | Mean snow density (kg m$^{-3}$) | Water equivalent (mm) |
|---|---|---|---|---|---|---|
| 1 | 2646 | 30-09-2009 | 21-11-2009 | -1.23 | 422 | 519 |
| 2 | 2828 | 02-10-2009 | 21-11-2009 | -0.81 | 441 | 357 |
| 3 | 2939 | 03-10-2009 | 21-11-2009 | -0.33 | 413 | 136 |

**Table 2: Mean monthly energy fluxes at AWS1**

| | Incoming shortwave radiation [W m$^{-2}$] | Net radiation [W m$^{-2}$] | Latent heat [W m$^{-2}$] | Sensible heat [W m$^{-2}$] | Melt energy [W m$^{-2}$] |
|---|---|---|---|---|---|
| October 2009 | 238 | 43 | -43 | 18 | 17 |
| November 2009 | 279 | 99 | -28 | 16 | 87 |
| December 2009 | 373 | 249 | -13 | 19 | 255 |
| January 2010 | 322 | 225 | -6 | 30 | 249 |

**Table 3: Monthly discharge from Universidad glacier as percentage of the total discharge in the Tinguiririca river, measured at the DGA station. Ranges in the percentages are for $F_{DH}$ ice values of 0.29 and 0.38 mm w.e. °C$^{-1}$ h$^{-1}$. Maximum and minimum are daily values.**

| Months | Monthly Mean | Monthly Max. | Monthly Min. |
|---|---|---|---|
| December 2009 | 4.3% - 5.2% | 5.6% - 7.0% | 3.0% - 3.7% |
| January 2010 | 8.1% - 10.2% | 13.0% - 16.5% | 4.5% - 5.6% |
| February 2010 | 14.1% - 17.9% | 25.7% - 32.5% | 7.5% - 9.5% |
| March 2010 | 15.3% - 19.5% | 26.6% - 33.9% | 5.4% - 7.0% |
| Mean of the period | 10.5% - 13.2% | 17.7% - 22.5% | 5.1% - 6.5% |
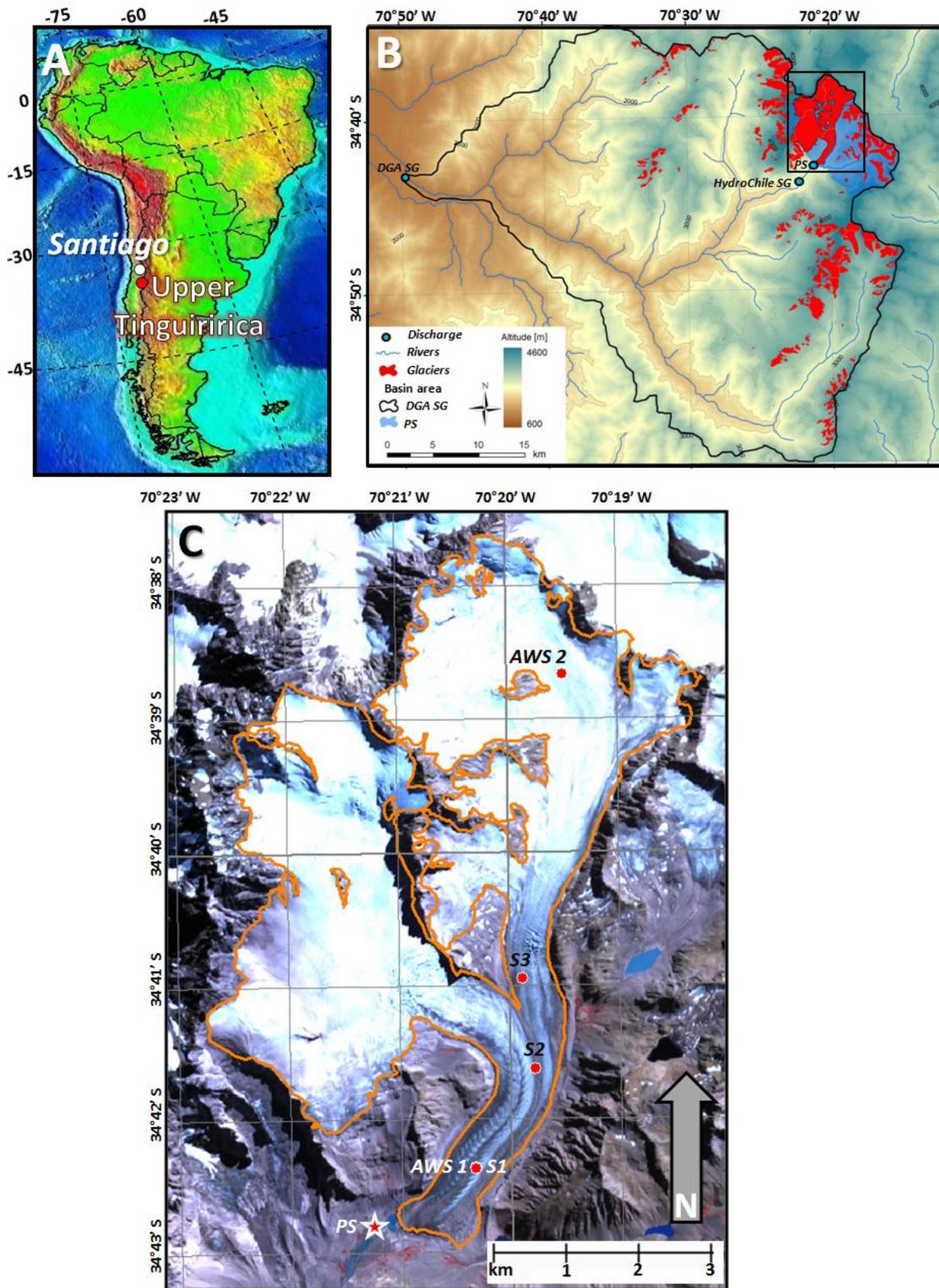
**Figure 1: Location of the Universidad glacier in central Chile. Panel A shows the regional location, Panel B shows the entire upper Tinguiririca basin and panel C shows Universidad glacier (orange outline), automatic weather stations (AWS) and ablation stakes (S) installed. PS indicates the location of the pressure sensor, SG indicates the location for stream gauge of DGA and HydroChile. The background is an ASTER image from 27 March 2010, UTM 19S.**
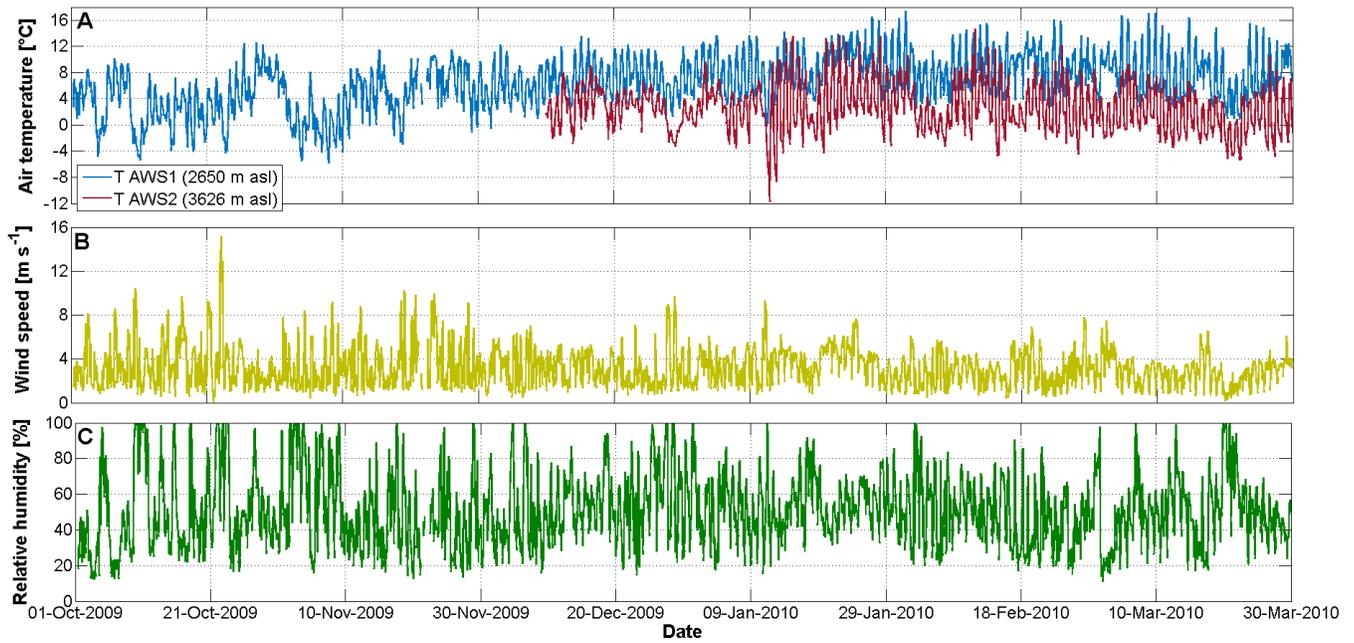
**Figure 2: Time series of hourly meteorological variables observed. A) Air temperature at AWS1 and AWS2, B) Wind speed at AWS1 and C) Relative humidity at AWS1.**
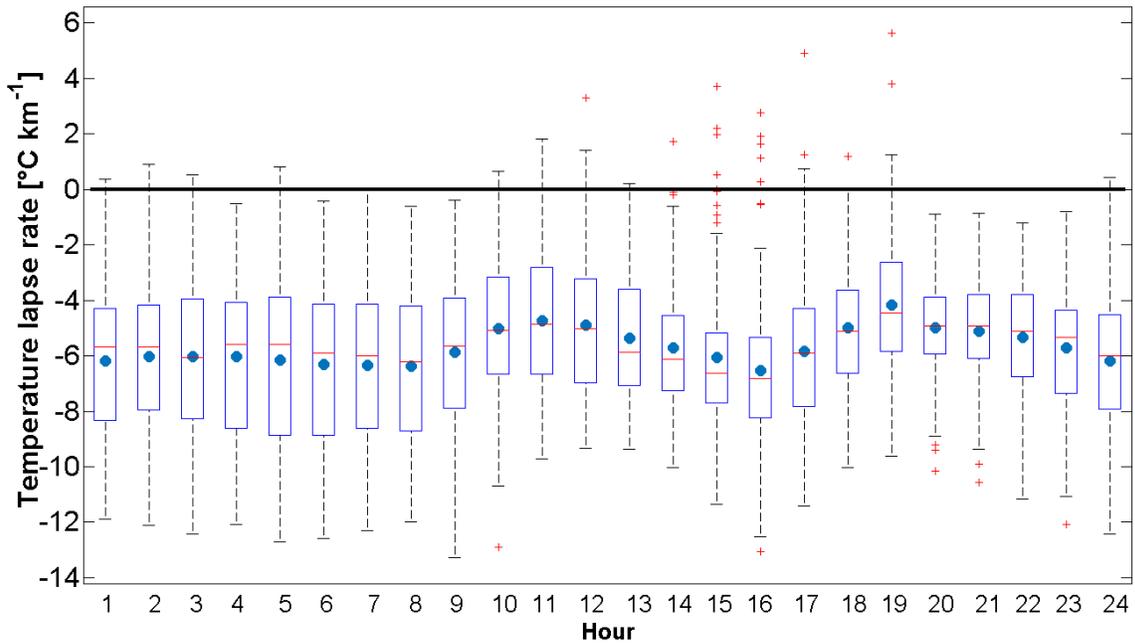
**Figure 3: Boxplot showing the statistical distribution of hourly lapse rate calculated between AWS1 and AWS2 in the common period. Upper and lower box limit are the 75% and 25% quartiles, the red horizontal line is the median, the fill circle is the mean, crosses are outlying values.**
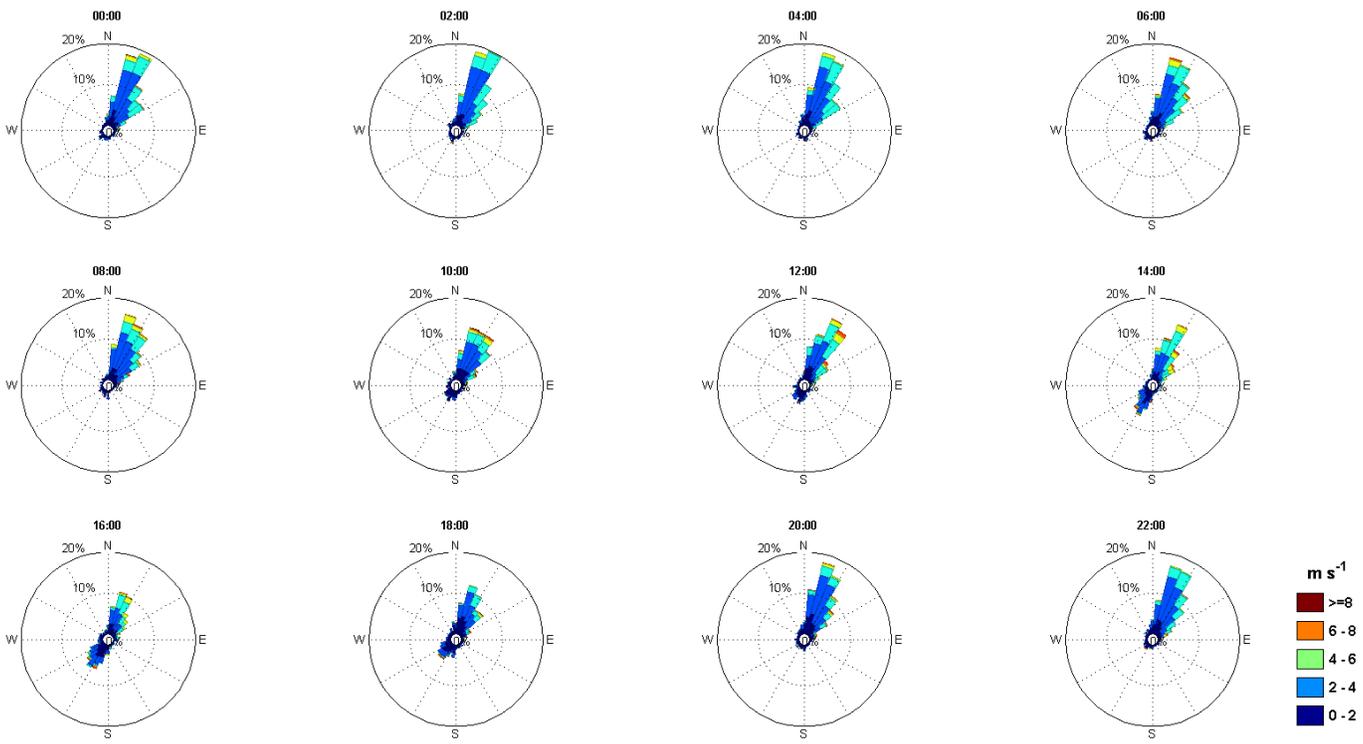
**Figure 4: Hourly wind roses showing the predominant wind direction and the wind speed at AWS1 (local time).**
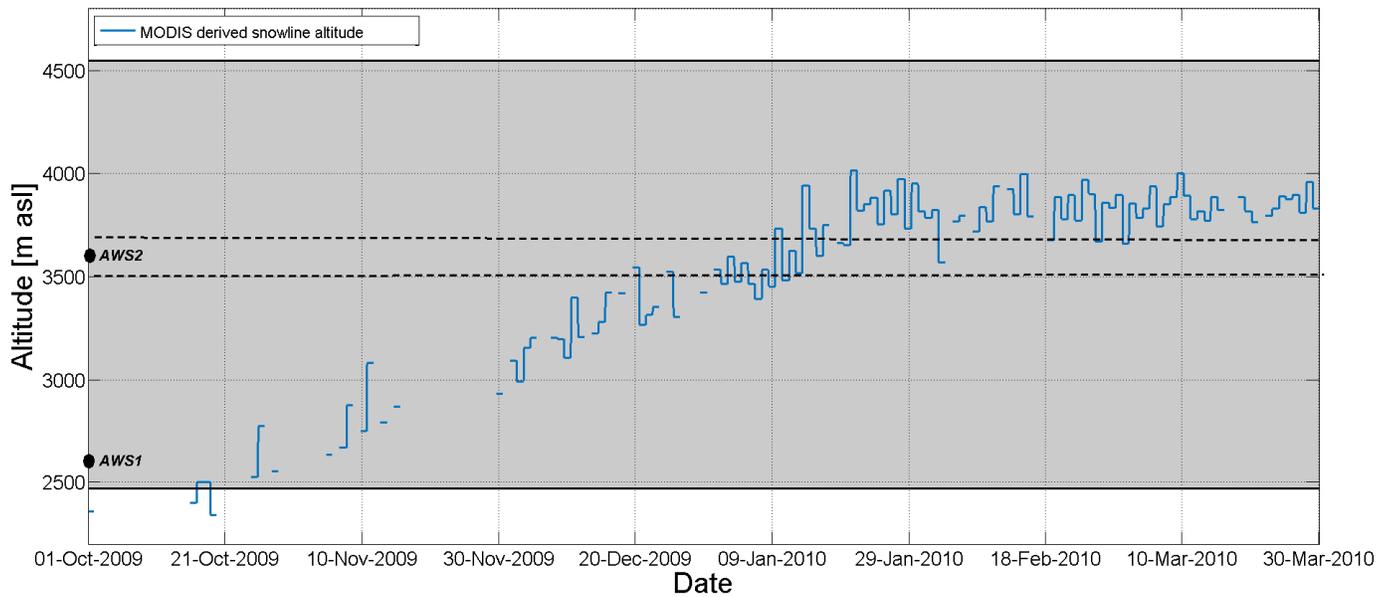
5 **Figure 5: Snow line elevation estimated using the MODIS snow product. The grey area corresponds to the altitude range of Universidad glacier, dashed line shows the Equilibrium Line Altitude range estimated using an ASTER image and black points show the AWS elevations.**
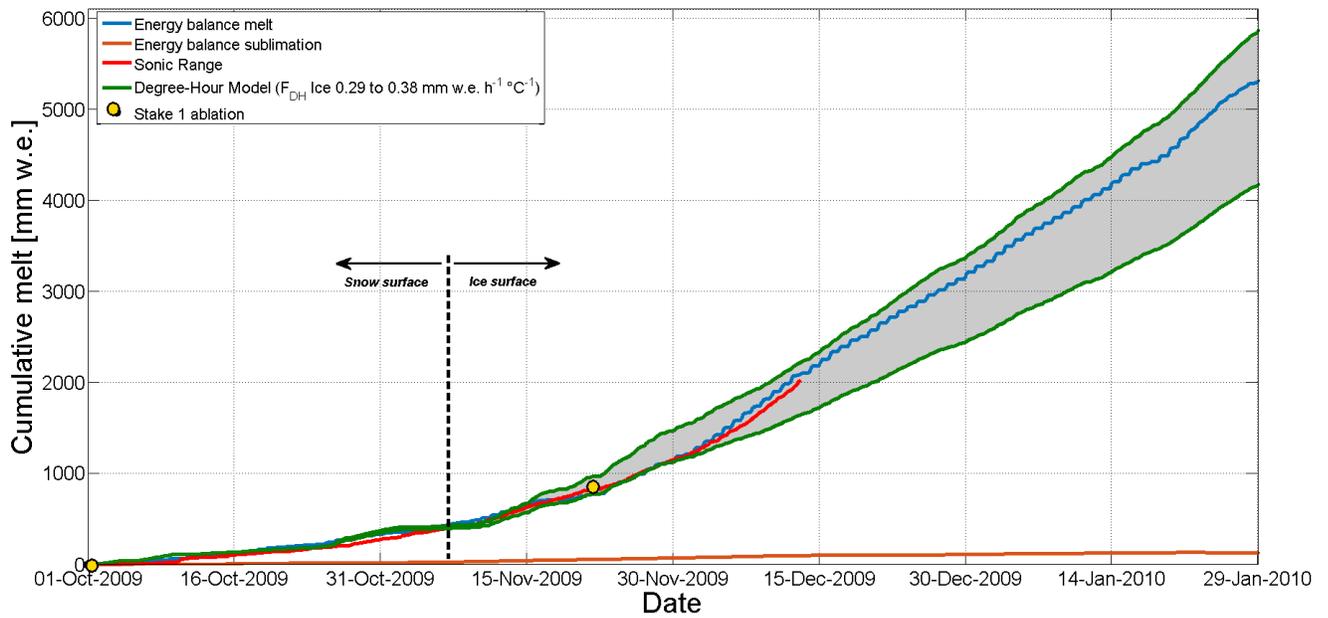
**Figure 6: Comparison of cumulative melt estimated by the point scale degree-hour model (grey area), point scale energy balance model, sonic ranger and stake 1 located near the AWS1 (2650 m asl).**
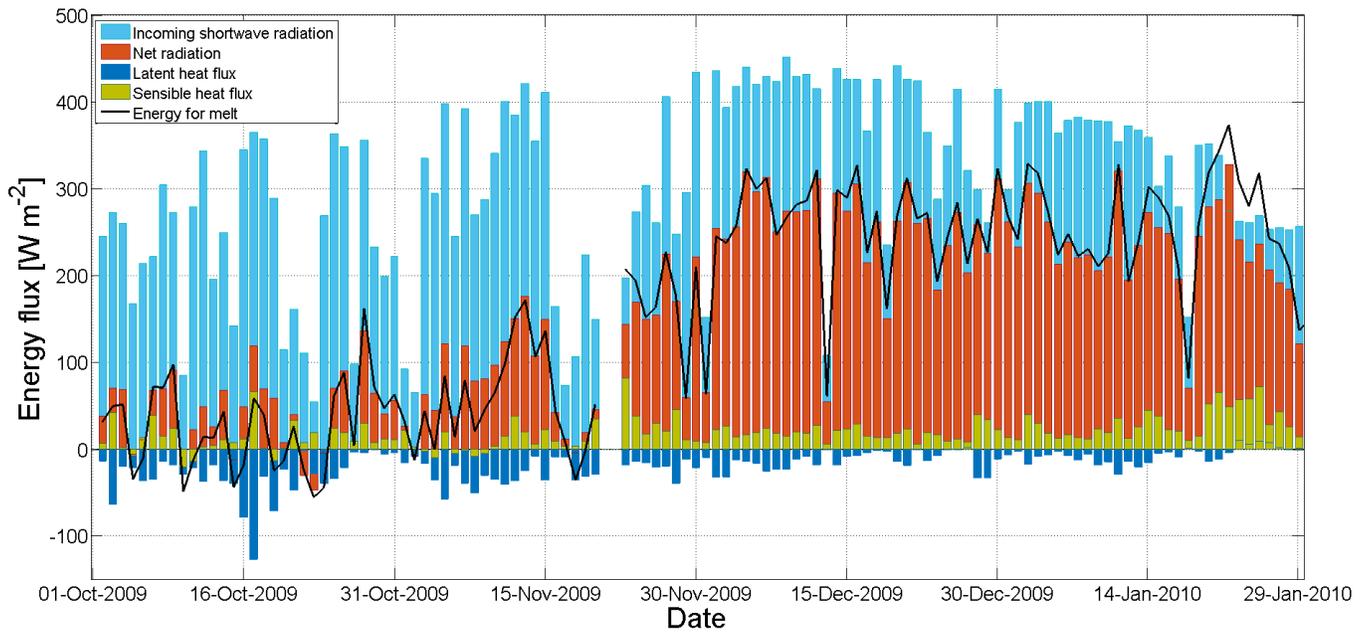
**Figure 7: Daily mean net radiation, incoming shortwave radiation, latent and sensible heat fluxes and the calculated energy available for melt at AWS1 (2650 m asl). On 21 and 22 November there is no data due to maintenance of the AWS1.**
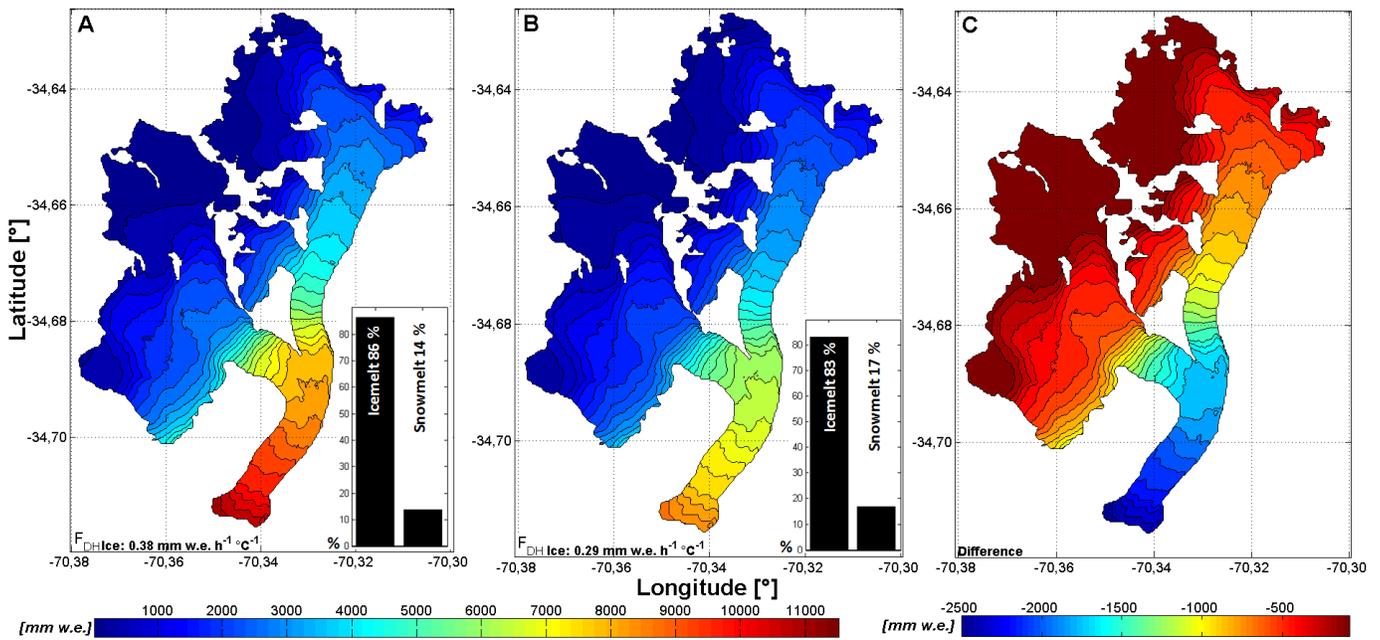
**Figure 8: Spatial distribution of cumulative glacier melt for Universidad glacier using two different $F_{DH}$ values for ice. A) $F_{DH}$ 0.38 mm w.e. h$^{-1}$ °C$^{-1}$, B) $F_{DH}$ 0.29 mm w.e. h$^{-1}$ °C$^{-1}$ and C) Difference. Totals for October 2009 to March 2010 period.**
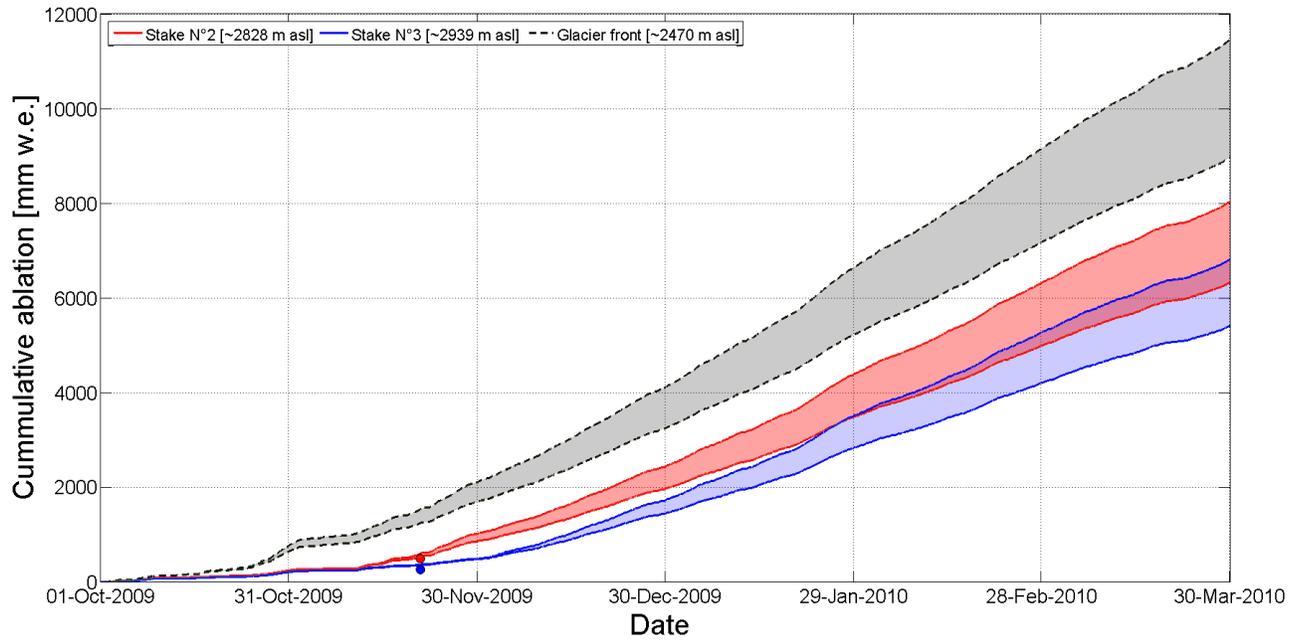
**Figure 9: Total cumulative melt of Universidad glacier using the degree-hour model. The red and blue lines and areas represent the cumulative melt at the locations of stakes 2 and 3, respectively. Points indicate the stake measurements. The area in grey enclosed by dashed black lines represents the lowest altitude of the glacier.**
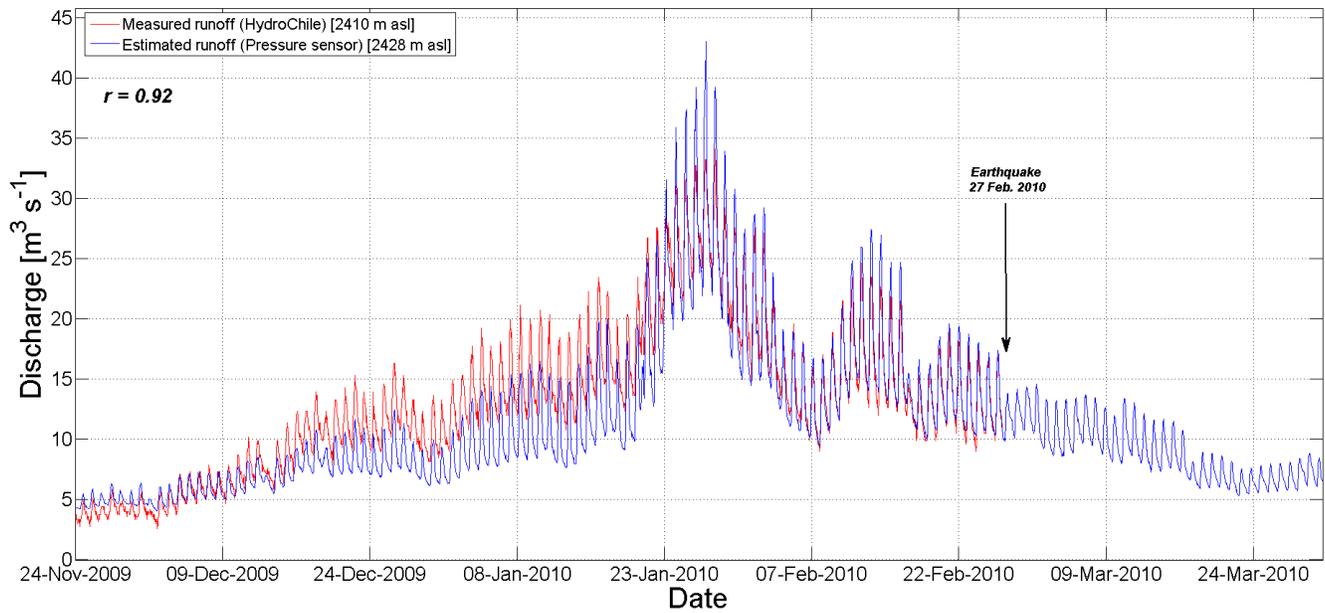
**Figure 10: Time series of hourly runoff in the proglacial stream from the water level pressure sensor and HydroChile gauging station.**
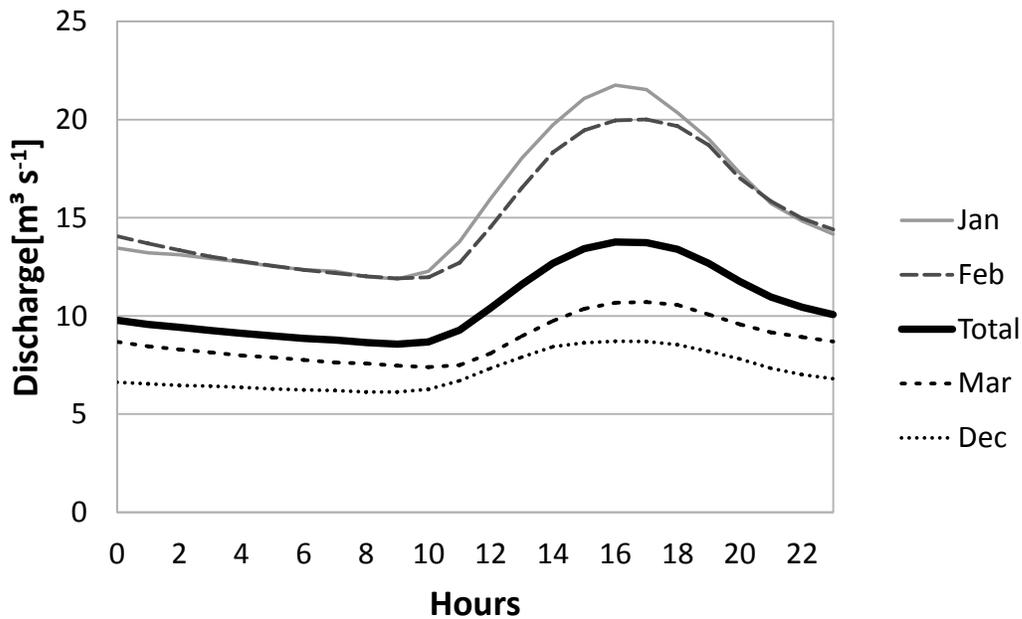
5    **Figure 11: Hourly mean discharge during the total monitored period (black solid line) and for each month estimated from pressure sensor at 2438 m asl.**
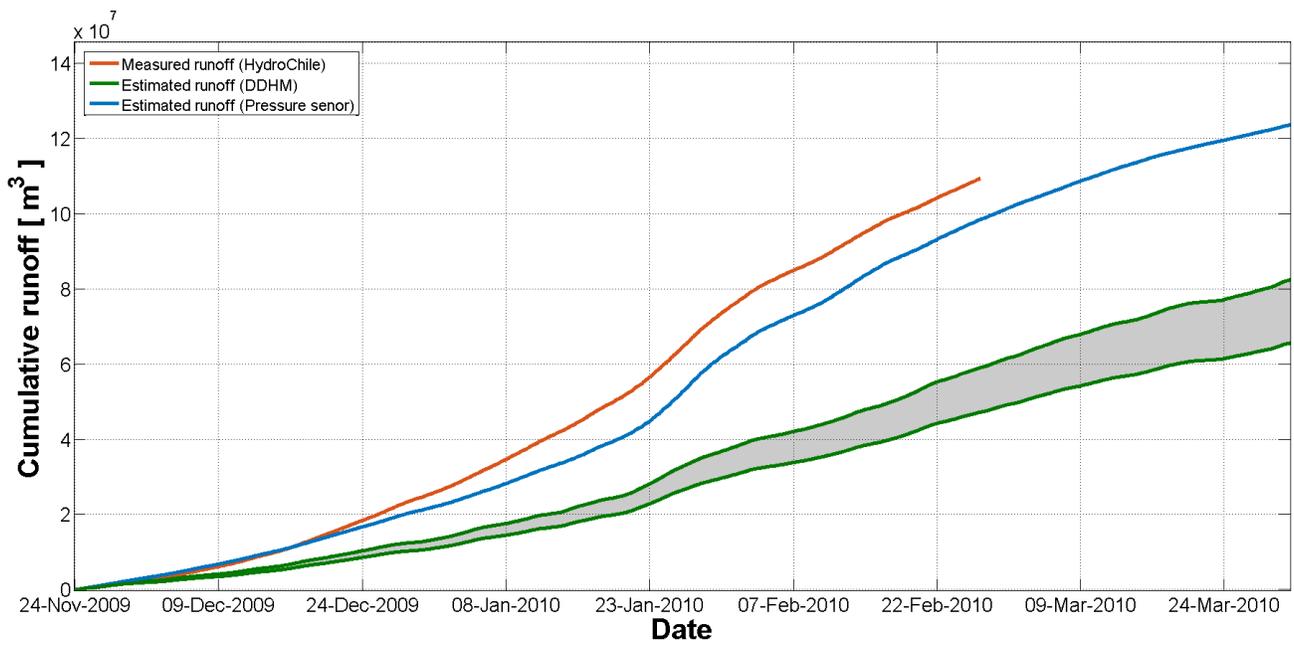
**Figure 12: Comparison of cumulative runoff calculated with distributed degree-hour model (grey area), and river runoff measurements from water level sensor data and the HydroChile station.**
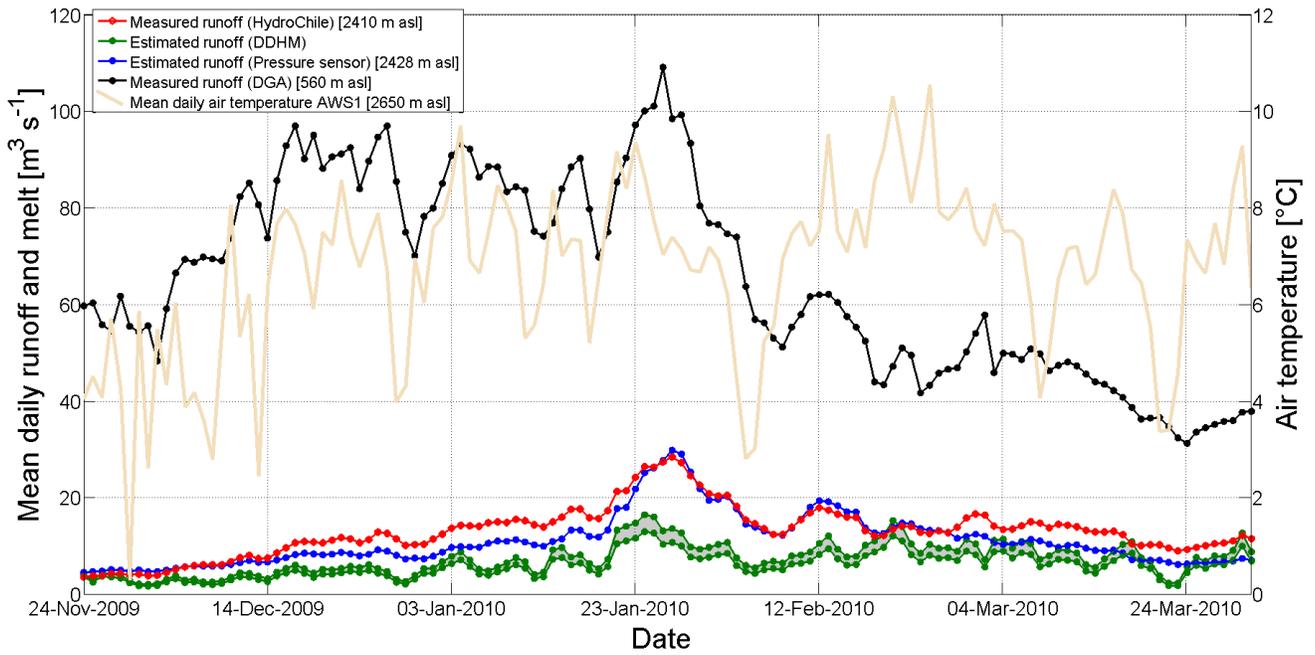
**Figure 13: Daily mean runoff from distributed degree-hour model, and river runoff measurements from water level sensor, HydroChile station and DGA station. For reference mean daily air temperature at AWS1 is plotted in right y axis.**